Stress and displacement around a crack in layered network systems mimicking nacre

Yuko Aoyanagi and Ko Okumura
Department of Physics, Graduate School of Humanities and Sciences, Ochanomizu University, 2-1-1, Otsuka, Bunkyo-ku, Tokyo 112-8610, Japan

(Received 24 September 2008; published 17 June 2009)

Nacre is a natural composite material which has been studied because of its remarkable structure and its strength. In this paper, we revisit a layered model of nacre proposed previously [K. Okumura and P. G. de Gennes, Eur. Phys. J. E **4**, 121 (2001)] in order to understand the physical reasons for the toughening via numerical simulation. We construct a two-dimensional lattice model which reflects the layered structure and perform a numerical study. This grid model reproduces the essential features predicted by the analytical solutions to the previous model and the results elucidate the reasons why the tip-stress concentration is reduced and tip displacement is enhanced in the layered system.

DOI: 10.1103/PhysRevE.79.066108 PACS number(s): 46.50.+a, 87.85.jc, 81.07.Pr, 62.25.Mn

The shiny beautiful material on the surface of pearls or inside walls of certain seashells is called *nacre*, which is known to posses a remarkable toughness [1,2] and has attracted a considerable attention [3–7]. In nacre, hard sheets are glued by thin soft sheets on submicron scale to form a *layered structure*. As a matter of fact, each hard sheet is composed of polygonal thin plates; the plate itself is composed of nanograins embedded in soft matrix [8]. Due to this rather complex structure various mechanisms have been proposed: the stepwise elongation of adhesive fibers [9], a threshold strength originating from thin compressive layers [10], the reduction in crack-tip-stress concentration [11], the pull-out resistance opposing to roughness of layer interfaces [12], the presence of mineral bridges between the aragonite platelets [13], and the microscale waviness of the plates [14]. Various theoretical and computational approaches include elastic [10,11,15] and viscoelastic models [16], micromechanical [17] and finite-element models [14,18,19], a fuse network model [20], and so forth.

In this paper, we consider a layered model of nacre (Fig. 1) proposed in [11], ignoring complex structures beyond the layered structure. For this model, analytical solutions for crack problems are obtained for a few cases [11,21], from which one possible mechanism of toughening of nacre has emerged: crack-tip stress is reduced while crack-tip displacement is increased. However, physical reasons for the reduction and increase have not been elucidated. Here, in order to clarify the physical pictures for them, we construct and study a two-dimensional network model.

In the analytical model (Fig. 1), hard layers (thicknesses d_h and Young modulus E_h) are glued together by soft layers (thicknesses d_s and Young modulus E_s) where the period of stripe d is defined as $d=d_s+d_h$. In nacre, we expect that the small parameters ε_E and ε_d ($E_s \equiv \varepsilon_E E_h$, $d_s \equiv \varepsilon_d d_h$) satisfy the condition

$$\varepsilon \equiv \varepsilon_E d/d_s \cong \varepsilon_E/\varepsilon_d \cong (E_s/E_h)(d/d_s) \ll 1. \tag{1}$$

By focusing on the leading-order contributions in the ε expansion of the elastic energy, we showed [11,22] that, for a line crack running in the x direction [as in Figs. 1(a) and 1(b)] under the plane strain condition (thick plate), the dominant component of the displacement field is the y component (u_y) which satisfies a *reduced* Laplace equation,

$$\left(\frac{\partial^2}{\partial \hat{x}^2} + \frac{\partial^2}{\partial y^2}\right) u_y = 0, \tag{2}$$

where the reduced x coordinate, $\hat{x} \equiv x/\sqrt{\varepsilon}$, has been introduced. The boundary value problems of this equation have been solved for a semi-infinite line crack [Fig. 1(a), [11,23]] and for a finite crack of length a [Fig. 1(b), [21,24]] in an infinitely long (thick) plate of width L. In the latter case the appropriate fixed-grip boundary conditions in the upper half plane ($y>0$) are as follows:

$$u_y = u_0 \quad \text{at} \quad y = L/2,$$

$$u_y = 0 \quad \text{for} \quad y = 0, \quad x < -a/2 \quad \text{or} \quad x > a/2,$$

$$\partial_y u_y = 0 \quad \text{for} \quad y = 0, \quad -a/2 < x < a/2. \tag{3}$$

In both cases the original field u_y has a discontinuous jump at the crack surface [e.g., $x<0$, $y=0$ in Fig. 1(a)]: u_y is positive for $y=0^+$ but negative for $y=0^-$. This singularity can be avoided by considering an auxiliary field and analytical solutions are obtained in [11,21]. For example, for the fixed-grip boundary conditions in Eq. (3), we obtain compact expressions for tip stress and tip displacement. In particular, in the limit, $L \ll \hat{a} \equiv a/\sqrt{\varepsilon}$, which includes the case $L \simeq a$, the displacement at $x=a/2-r$ and the stress at $x=a/2+r$ are given by

$$u_y(x = a/2 - r, y = 0^+) = 2\varepsilon^{-1/4} K_L \sqrt{r}/E_h,$$

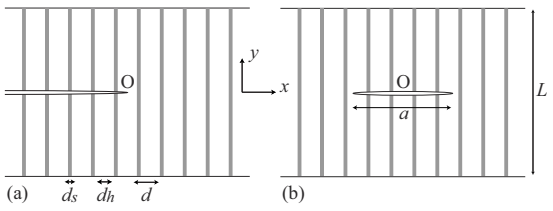

FIG. 1. Layered structure (a) with a semi-infinite crack and (b) with a finite crack. In (b), the right crack tip is located at $(x,y)=(a/2,0)$. Gray stripes correspond to soft thin layers.

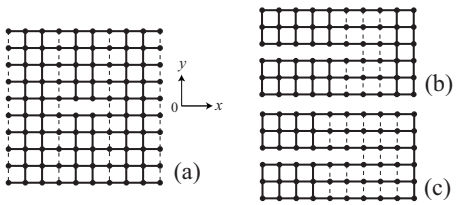

FIG. 2. (a) The illustration of lattice model with a crack in the middle to be stretched in the y direction, where $d_s=l_0$, $d=3l_0$, $a=3l_0$; the dashed line stands for the weaker spring. The fracture tips are located at the soft "layer." (b) and (c) Magnified view of the right crack tip located in the middle of soft layer with $d_s=3l_0$ and $d_s=5l_0$, respectively $(d,a \gg d_s)$.

$$\sigma_{yy}(x=a/2+r,y=0^+)=\varepsilon^{1/4}K_L/\sqrt{r}, \tag{4}$$

where $K_L \equiv \sigma_0\sqrt{L/(2\pi)}$ is the stress intensity factor in the nonlayered case [25]; r and $\sigma_0 \equiv E_h u_0/L$ measure the distance from the tip and the remote stress, respectively. In the two equations in (4), the tip displacement is enhanced by a factor $\varepsilon^{-1/4}$ while tip-stress concentration is reduced by a factor $\varepsilon^{1/4}$ compared with the nonlayered case. For the boundary value problem indicated in Fig. 1(a), we obtain the same scaling relation around the crack tip [11]. This is natural because in both problems the only length scales available are $L \simeq a$ and r [24].

As indicated above, we shall construct a two-dimensional grid model for numerical studies (Fig. 2) which reproduces the tendency stipulated in the two equations in (4). In this problem, we have several well-separated length scales: strictly speaking, we must satisfy the relations

$$d_s \ll d_h(\simeq d) \ll r \ll a(\simeq L) \ll L_x, \tag{5}$$

where L_x is the system size in the x direction. In the following, to ease the calculational burden we relax this condition; below we set the separation between two adjacent variables in Eq. (5) less than 1 order of magnitude. Nonetheless, we will see that this relaxation is allowed to attain our goals: reproduction of the tendency and elucidation of the physical pictures.

The two-dimensional grid model is composed of $M \times N$ points, initially arranged in a two-dimensional square lattice (Fig. 2), with each point $\mathbf{X}_{ij}$ connected to the four nearest neighbors $\mathbf{X}_{ij}^{(s)}$,

$$\mathbf{X}_{ij}^{(s)}=\begin{cases}\mathbf{X}_{i+1j} & (s=1)\\ \mathbf{X}_{ij+1} & (s=2)\\ \mathbf{X}_{i-1j} & (s=3)\\ \mathbf{X}_{ij-1} & (s=4),\end{cases} \tag{6}$$

with a linear spring of natural length l_0. The four springs attached to a point (i,j) provide force reflecting the layered structure whose α (x or y) component is given by

$$F_{i,j,\alpha}=\sum_{i=1}^{M}\sum_{j=1}^{N}\sum_{s=1}^{4}k(i,j,s)(\mathbf{X}_{i,j}^{(s)}-\mathbf{X}_{i,j}-\boldsymbol{l}^{(s)})_\alpha, \tag{7}$$

where

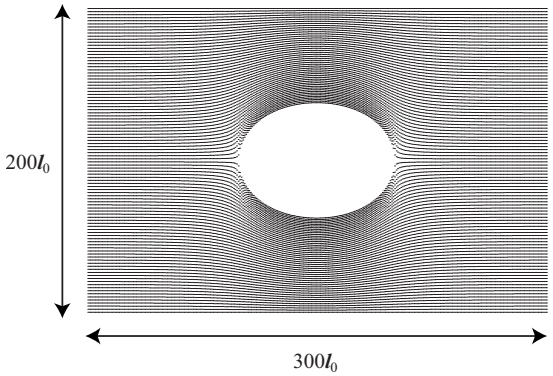

FIG. 3. The reference nonlayered network at equilibrium of original size, $(L,L_x)=(100l_0,300l_0)$, with a crack of length $a=101l_0$, stretched to $200l_0$ in the y direction.

$$\boldsymbol{l}^{(s)}=\begin{cases}(l_0,0) & (s=1)\\ (0,l_0) & (s=2)\\ (-l_0,0) & (s=3)\\ (0,-l_0) & (s=4).\end{cases} \tag{8}$$

The spring constants $k(i,j,s)$ are set to constant k_h or $k_s=(E_s/E_h)k_h<k_h$ to reflect the desired layered structure [see Fig. 2(a)] while the special care is required for this setting at the boundary (e.g., j is either 1 or N) to realize the fixed-grip condition. A pseudoline crack of length $a=(n+1)l_0$ is introduced into the network by cutting n bonds in the middle $(y=0)$, i.e., by setting $k(i,j,s)$ to zero at corresponding points ($j=N/2$ for $s=2$ and $j=N/2+1$ for $s=4$ for even N). For technical convenience, we set the crack tips in the middle of soft layers (see Fig. 2) although, qualitatively, results below are not sensitive to this choice. The network with the crack thus introduced is stretched in the y direction so that the displacement at upper and lower ends, initially located at $y=\pm L/2$, is $\pm eL/2$ (see Fig. 3 for the nonlayered system).

The equilibrium force distribution as in Fig. 3 is obtained via numerical calculations by solving coupled equations of motions,

$$\eta\frac{dX_{ij\alpha}}{dt}=F_{i,j,\alpha}. \tag{9}$$

The dynamics can be relaxed to a unique equilibrium state after a sufficient time t. The damping constant η changes only the dynamical process to reach the equilibrium state: results below are insensitive to η.

A similar but nonlayered model composed of nonlinear springs is discussed recently in [26,27]. In [26] the x and y components of $\mathbf{X}_{i,j}$ vector are coupled. On the contrary, in the present model, the x and y components are independent so that the interdistance between the adjacent points $\mathbf{X}_{i,j}$ in the x direction is always fixed to l_0; this might seem to be an oversimplification but has strong advantages: e.g., the x coordinate of tip position is always fixed to the original position, which technically eases the interpretation without changing the physical tendency.

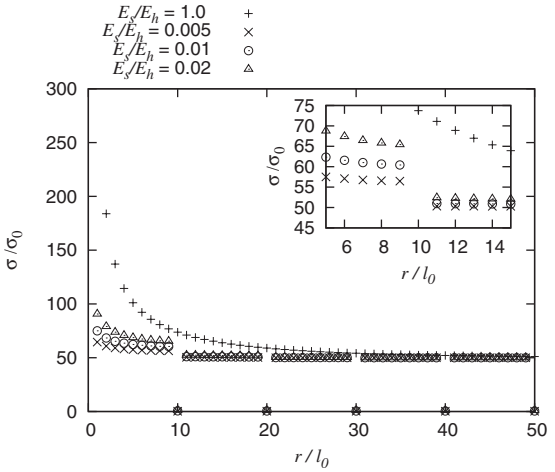

FIG. 4. Stress distribution around the crack at $y=l_0/2$ for various E_s/E_h with $d=10l_0$ and $d_s=l_0$. The crack is located at $y=0$ and the right crack tip is located at $x=a/2$; here, the distance from the tip r is defined as $r=x-a/2$.

To demonstrate that our lattice model can reproduce the original tendency in the two equations in (4), we show the result of stress and deformation in Figs. 4–7 for a system with $L_x=300l_0$, $L=100l_0$, and $a=101l_0$ for various d_s, d, and E_s/E_h to change ε given in Eq. (1). In all plots, stress and displacement are those for the beads located at $y=l_0/2$ before stretch, while the crack is introduced by cutting 100 springs located at $y=0$ (i.e., spring connecting the beads originally located at $y=\pm l_0/2$).

The continuous curves for $E_s/E_h=1$ or $d_s/d=0$ correspond to the nonlayered case (all springs are set to k_h), which are references for stress reduction and displacement increase. As expected, these reference lines for stress and displacement qualitatively reproduce the well-known $1/\sqrt{r}$ and $\sqrt{r}$ profiles, respectively [25,28]. In the layered cases, all the curves are singular in the regions of soft layers: the stress curves are dropped sharply at the "soft layers," while the displacement curves make "discontinuous jumps" at the soft layers; the curves for "layered grid model" are intermittent but the "envelope curves" or "overall profiles" reproduce the tendency in the two equations in (4)—as ε in Eq. (1) gets smaller, the stress concentration profiles and the displacement profiles in layered cases are reduced and augmented

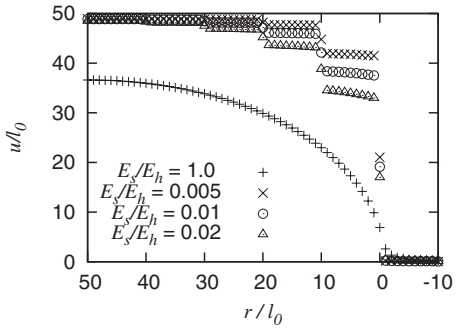

FIG. 5. Tip displacement around the crack at $y=l_0/2$ and for various E_s/E_h with $d=10l_0$ and $d_s=l_0$. Here, the distance from the tip r is defined as $r=a/2-x$.

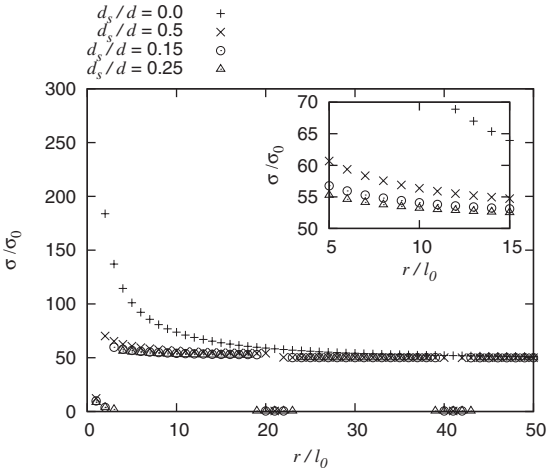

FIG. 6. Stress distribution around the crack at $y=l_0/2$ for various d_s/d with $d=20l_0$ and $E_s/E_h=100$, where $r=x-a/2$.

from the corresponding nonlayered continuous curves, respectively; and this is confirmed by changing ε in two different ways, i.e., by varying E_s/E_h with d/d_s fixed (Figs. 4 and 5) and vice versa (Figs. 6 and 7). Note here that we expect that the grid model approaches the continuum model under the condition given in Eq. (5).

Now that we have confirmed that our naive calculations capture the tendency of the original analytical model, we can discuss the physical picture of the stress reduction and displacement enhancement predicted by analytical solution based on these plots: the displacement enhancement in the layered system clearly comes from the large deformation of the soft springs in the meshed system. This implies that the hard springs are less deformed, which leads to the reduction in stress because overall stress σ_{yy} is governed by the hard layers: $\sigma_{yy}\sim E_h e_h$ for $d_h \gg d_s$ where e_h is the strain in the hard layers. This picture based on the grid model elucidates the analytical behavior in the continuum limit, as announced.

These pictures are independent of the details in setting numerical calculation. For example, we changed the position of tip, slightly within the soft layers or even outside to the hard layers, to find that these changes do not cause any qualitative differences [29]; we made the amount of stretch smaller (about 1/10) and changed the system size to find no qualitative changes. In addition, to confirm that our result is not affected by the anisotropy of the square lattice (this is

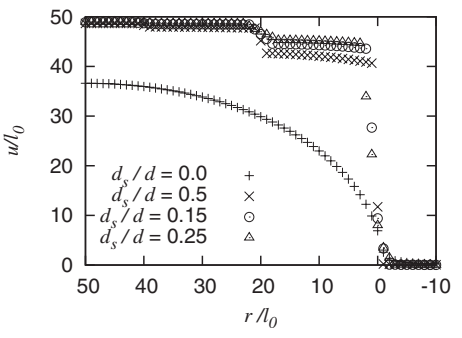

FIG. 7. Displacement around the crack at $y=l_0/2$ for various d_s/d with $d=20l_0$ and $E_s/E_h=100$, where $r=a/2-x$.

important in some cases, e.g., [30]), we performed simulation with a square lattice lying at 45° from the layers to find essentially the same results as above. In this sense, our qualitative understanding is robust.

The numerical model in this paper is based on the analytical layered model *mimicking* nacre introduced in [11]. As stated before, this original model does not reflect more detailed structure: an infinite hard layer in the analytical model is, in reality, a collection of hexagonal plates, which consist of grains, etc. However, it is still interesting to see how the original model compare with the real nacre [quantitative comparison directly with the present numerical model is not appropriate since we relaxed the required condition in Eq. (5) for realistic calculations]; the correct order of magnitude of the fracture energy can be reproduced from the model if we assume that the soft layer is like a standard soft gel ($E_s \simeq 1$ MPa) [11], in which case the ε parameter is around 1/5000. This semiquantitative agreement encourages us to expect that the simple analytical model captures one of the essential toughening mechanisms of real nacre so that the present paper dealing with a corresponding numerical model offers physical reasons for toughening of real nacre. At any rate, the present study gives some insight on and a guide for toughening of artificial layered materials motivated by nacre.

Here, we should mention that there has been a controversy on the estimation of E_s. In [2], they assumed $E_s = 4$ GPa, an experimental value of keratin, because the direct measurement was impossible to explain their data on nacre as a composite material. Since then some researchers have used this value in their papers (e.g., [31]). On the contrary, many magnified photographs of the soft layer have indicated that the soft layer is like a gel (see, for example, a recent paper on *in situ* experiments [32]), for which the standard value in polymer physics is $E_s \simeq 1$ MPa [33]. In addition, in a recent study [34], the authors derived an even smaller value $E_s \simeq 100$ Pa from deflection experiment. Overall, this controversial situation over two decades shows the difficulty in determining E_s. Note that our theory as a model of nacre can be acceptable almost in any cases because the required condition $\varepsilon < 1$ is satisfied if $E_s <$ a few gigapascals.

We state that the continuous curves for $E_s/E_h = 1$ or $d_s/d = 0$ correspond to the nonlayered case because in such a case the network becomes homogeneous consisting of only one kind of spring. However, the continuous numerical curves shown in the above where $E_s/E_h = 1$ or $d_s/d = 0$ do not coincide with the curves calculated from the analytical solution (although we confirmed that they agree quite well if we introduce a numerical prefactor); this is because the mathematical limit matching with the analytical solution is the limit $\varepsilon \to 1$ with letting E_s/E_h and d/d_s closer to zero and infinity, respectively.

To better understand the physics of our results, it is quite interesting to compare our result with those in the context of a version of shear-lag models [35]. This two-dimensional model for a composite consists of strong fibers sandwiched by matrix with the following restriction: tension of the composite is supported only by fibers while shear is carried only by the matrix (a similar idea is also found in [5]). Looking back our results of simulation, we notice that soft layers are strongly sheared while hard layers are stretched (rather than sheared). The restriction set by hand in the shear-lag model seems to be realized naturally (without setting by hand) to a certain degree in our numerical results. At this level of a rough understanding, our soft modulus E_s can be practically regarded as a shear modulus while E_h as a Young modus (we cannot define the Poison ratio in an unambiguous way in our model). By the way, in [36] the authors compared, in the context of the shear-lag model, a continuum treatment with a discrete one, which is similar in spirit to the present work; they discuss the position of the crack tip in the soft matrix and indicate a best position in agreement to the continuum treatment (in our case since our discrete model is a finite system, contrary to theirs, this kind of qualitative comparison is impossible).

To reflect real scales in nacre, L is around several centimeters while significant sizes (a) of crack fatal to nacre would range from submillimeter (note that our model is applicable when $a \gg d$) to a few centimeters: L/a ranges from 1 to 100. In our simulation the ratio is very restricted, on the order of 1 (i.e., 1 or 3); however, it would be interesting to compare our numerical results in the case of $L = 3a$ and those in the case of $L = a$. Basically, we think that our numerical results for $L/a = 1$ and 3 correspond to the limit $L \simeq a$ of the analytical solution obtained in [21], in which another limit of $L \gg a$ is also considered; comparing these two limits of the analytical solutions, we can conclude that the reduction in the stress concentration is weakened as L gets larger, which is consistent with the comparison of the cases $L/a = 1$ and 3 of our numerical results. Studying the cases of larger ratio L/a and comparing the results with the previous works in the shear-lag model [36,37] would be interesting, which will be discussed elsewhere.

In conclusion, we have succeeded in developing a layered grid model for the previous analytical model mimicking nacre; the grid model reproduces the important features [two equations in (4)] of the original analytical model. The resultant stress and displacement distributions in the grid model give physical insights on the reason of the reduction in the stress concentration and displacement enhancement due to the layered structure: strong deformation in the soft layers increases the overall displacement field, which in turn relaxes the deformation in the hard layers to reduce the stress concentration since continuous stress field σ_{yy} is essentially governed by the hard modulus: $\sigma_{yy} \sim E_h e_h$ for $d_h \gg d_s$.

The authors thank Hideki Kakisawa (NIMS, Japan) for informative discussions. This work was supported by KAKENHI from MEXT, Japan.

[1] J. D. Currey, Proc. R. Soc. London, Ser. B **196**, 443 (1977).
[2] A. P. Jackson, J. F. V. Vincent, and R. M. Turner, Proc. R. Soc. London, Ser. B **234**, 415 (1988).
[3] M. Sarikaya and I. A. Aksay, *Nacre: Properties, Crystallography, Morphology, and Formation in Biomimetics: Design and Processing of Materials* (AIP, New York, 1995).
[4] S. Kamat, X. Su, R. Ballarini, and A. H. Heuer, Nature (London) **405**, 1036 (2000).
[5] H. J. Gao, B. H. Ji, I. L. Jager, E. Artz, and P. Fratzl, Proc. Natl. Acad. Sci. U.S.A. **100**, 5597 (2003).
[6] G. Mayer, Science **310**, 1144 (2005).
[7] S. Deville, E. Saiz, R. K. Nalla, and A. P. Tomsia, Science **311**, 515 (2006).
[8] X. D. Li, W. C. Chang, Y. J. Chao, R. Z. Wang, and M. Chang, Nano Lett. **4**, 613 (2004).
[9] B. L. Smith, T. E. Schaeffer, M. Viani, J. B. Thompson, N. A. Frederick, J. Kindt, A. Belcher, G. D. Stucky, D. E. Morse, and P. K. Hansma, Nature (London) **399**, 761 (1999).
[10] M. P. Rao, A. J. Sanchez-Herencia, G. E. Beltz, R. M. McMeeking, and F. F. Lange, Science **286**, 102 (1999).
[11] K. Okumura and P. G. de Gennes, Eur. Phys. J. E **4**, 121 (2001).
[12] A. G. Evans, Z. Suo, R. Z. Wang, I. A. Aksay, M. Y. He, and J. W. Hutchinson, J. Mater. Res. **16**, 2475 (2001).
[13] F. Song and Y. L. Bai, J. Mater. Res. **18**, 1741 (2003).
[14] F. Barthelat, C.-M. Li, C. Comi, and H. D. Espinosa, J. Mater. Res. **21**, 1977 (2006).
[15] K. Okumura, Eur. Phys. J. E **7**, 303 (2002).
[16] K. Okumura, Europhys. Lett. **63**, 701 (2003).
[17] S. P. Kotha, Y. Li, and N. Guzelsu, J. Mater. Sci. **36**, 2001 (2001).
[18] D. R. Kattii, K. S. Katti, J. M. Sopp, and M. Sarikaya, Comput. Theor. Polym. Sci. **11**, 397 (2001).
[19] B. Ji and H. Gao, J. Mech. Phys. Solids **52**, 1963 (2004).
[20] Phani Kumar V. V. Nukala and S. Šimunović, Phys. Rev. E **72**, 041919 (2005).
[21] Yukari Hamamoto and Ko Okumura, Phys. Rev. E **78**, 026118 (2008).
[22] K. Okumura, J. Phys.: Condens. Matter **17**, S2879 (2005).
[23] Yukari Hamamoto and Ko Okumura, J. Eng. Mech. **135**, 461 (2009).
[24] K. Okumura (unpublished).
[25] T. L. Anderson, *Fracture Mechanics-Fundamentals and Applications* (CRC, Boca Raton, 1991).
[26] S. Nakagawa and K. Okumura, J. Phys. Soc. Jpn. **76**, 114801 (2007).
[27] Y. Aoyanagi and K. Okumura, J. Phys. Soc. Jpn. **78**, 034402 (2009).
[28] K. Okumura, Europhys. Lett. **67**, 470 (2004).
[29] In fact, in Figs. 6 and 7 the tips are located in the middle of soft layers as in Fig. 2 while they are shifted by one mesh outward in Figs. 4 and 5.
[30] B. Skjetne, T. Helle, and A. Hansen, Phys. Rev. Lett. **87**, 125503 (2001).
[31] F. Song, A. K. Soh, and Y. L. Bai, Biomaterials **24**, 3623 (2003).
[32] T. Sumitomo, H. Kakisawa, Y. Owaki, and Y. Kagawa, J. Mater. Res. **23**, 3213 (2008).
[33] M. Rubinstein and R. H. Colby, *Polymer Physics* (Oxford University Press, New York, 2003).
[34] M. A. Meyers, A. Y. M. Lin, P. Y. Chen, and J. Muyco, J. Mech. Behav. Biomed. Mater. **1**, 76 (2008).
[35] J. M. Hedgepeth, NASA TN D-882, 1961 (http://ntrs.nasa.gov/archive/nasa/casi.ntrs.nasa.gov/19980227450_1998390164.pdf).
[36] I. J. Beyerlein, S. L. Phoenix, and A. M. Sastry, Int. J. Solids Struct. **33**, 2543 (1996).
[37] S. L. Phoenix and I. J. Beyerlein, in *Statistical Strength Theory for Fibrous Composite Materials*, edited by T. W. Chou, Comprehensive Composite Materials Vol. 1 (Pergamon, New York, 2000), Chap. 1.19, p. 519.